Inorg. Chem. **2006**, *45*, 2896–2902

Syntheses, Structures, Near-Infrared and Visible Luminescence, and Magnetic Properties of Lanthanide-Organic Frameworks with an Imidazole-Containing Flexible Ligand

Zheng-Hua Zhang,[†] You Song,[†] Taka-aki Okamura,[‡] Yasuchika Hasegawa,[§] Wei-Yin Sun,*[,†] and Norikazu Ueyama[‡]

Coordination Chemistry Institute, State Key Laboratory of Coordination Chemistry, Nanjing University, Nanjing 210093, China, Department of Macromolecular Science, Graduate School of Science, Osaka University, Toyonaka, Osaka 560-0043, Japan, and Material and Life Science, Graduate School of Engineering, Osaka University, Suita 565-0871, Japan

Received October 19, 2005

Reactions of tripodal ligand 1,3,5-tris(imidazole-1-ylmethyl)-2,4,6-trimethylbenzene (L) with lanthanide metal salts and triethyl orthoformate led to the formation of six bowl-like dinuclear compounds $[Ln_2(L)(HL)(NO_3)_6(HCOO)]\cdot 3CH_3OH$ (Ln = Gd **1**, Tb **2**, Dy **3**, Er **4**, Yb **5**, and Eu **6**). The single-crystal X-ray diffraction analysis revealed that six complexes are isomorphous and isostructural and that the dinuclear molecules are further connected by hydrogen bonds and π–π interactions, resulting in 3D channel-like structures. The luminescence properties have been studied, and the results showed that the Tb(III) (**2**) and Eu(III) (**6**) complexes exhibited sensitized luminescence in the visible region and their luminescence lifetimes in powder and DMSO-d_6 solution are in the range of milliseconds. The Yb(III) complex (**5**) emits typical near-infrared luminescence in DMSO-d_6 solution. Variable-temperature magnetic susceptibility measurements of **1**–**6** showed that complex **1** (Gd) is nearly a paramagnet and complexes **2** (Tb), **3** (Dy), and **4** (Er) show the ferromagnetic coupling between magnetic centers, whereas the depopulation of the Stark levels in complexes **5** (Yb) and **6** (Eu) leads to a continuous decrease in $\chi_M T$ when the sample is cooled from 300 to 1.8 K.

Introduction

In recent years, various metal−organic frameworks (MOFs) with specific topologies such as cagelike structures and honeycomb and interpenetrating networks have been obtained by the self-assembly of suitable transition-metal salts with rigid or flexible organic ligands.[1] On the other hand, the use of trivalent lanthanide cations for constructing MOFs has been a rapidly developing area in recent years because their unique luminescence properties are advantageous in applications such as fluoroimmuno-assays, light-emitting diodes, laser systems, and optical amplification for telecommunications. The lanthanide ions have narrow emission bands and relatively long (millisecond order) luminescence lifetimes as a result of transitions within the partially filled 4f shell of the ions, which are parity-forbidden transitions in principle. Complexes of Eu(III) and Tb(III), which show luminescence in the visible region, are the most employed for applications such as fluoroimmuno-assays and fluorescence microscopy.[2] To date, lanthanide complexes, which have emission bands ranging from 880 to 1550 nm in the near-infrared region, such as Nd(III), Yb(III), and Er(III), attract a great deal of interests.[3] The Nd(III) and Yb(III) complexes are promising probes for fluoroimmuno-assays and in vivo applications, because human tissue is relatively transparent to near-infrared

* To whom correspondence should be addressed. Address: Coordination Chemistry Institute, Nanjing University, Nanjing 210093, China. Telephone: 86-25-83593485. Fax: 86-25-83314502. E-mail: sunwy@nju.edu.cn.
[†] Nanjing University.
[‡] Graduate School of Science, Osaka University.
[§] Graduate School of Engineering, Osaka University.

(1) (a) Fiedler, D.; Leung, D. H.; Bergman, R. G.; Raymond, K. N. *Acc. Chem. Res.* **2005**, *38*, 351. (b) Férey, G.; Mellot-Draznieks, C.; Serre, C.; Millange, F. *Acc. Chem. Res.* **2005**, *38*, 217. (c) Zou, R.-Q.; Jiang, L.; Senoh, H.; Takeichi, N.; Xu, Q. *Chem. Commun.* **2005**, 3526.

(2) (a) Coates, J.; Sammes, P. G.; Yahioglu, G.; West, R. M.; Garman, A. J. *Chem. Commun.* **1994**, 2311. (b) Mayer, A.; Neuenhofer, S. *Angew. Chem., Int. Ed.* **1994**, *33*, 1044. (c) Yam, V. W.-W.; Lo, K. K.-W. *Coord. Chem. Rev.* **1998**, *184*, 157. (d) Montalti, M.; Prodi, L.; Zaccheroni, N.; Charbonniere, L.; Douce, L.; Ziessel, R. *J. Am. Chem. Soc.* **2001**, *123*, 12694. (e) Parker, D.; Dickins, R. S.; Puschmann, H.; Crossland, C.; Howard, J. A. K. *Chem. Rev.* **2002**, *102*, 1977. (f) Klink, S. I.; Hebbink, G. A.; Grave, L.; Peters, F. G. A.; Veggel, F. C. J. M. V.; Reinhoudt, D. N.; Hofstraat, J. W. *Eur. J. Org. Chem.* **2000**, 1923.

10.1021/ic0518071 CCC: $33.50
Published on Web 03/09/2006

light around 1000 nm. In optical telecommunication networks, erbium ions are actually being used as the active components in Er^{3+}-doped silica fiber amplifiers (EDFAs) with a wavelength of about 1550 nm, which corresponds to an optical transition of Er^{3+} ($^4I_{13/2} \rightarrow {}^4I_{15/2}$ transition).

In addition, the large unquenched orbital angular momentum of most of lanthanide(III) ions associated with the internal nature of the valence f orbitals makes such ions very appealing for the preparation of magnetic materials. In fact, all the lanthanide ions, except gadolinium(III) and europium(II), have degenerate ground states that are split by spin−orbit coupling and crystal-field effects. Thus, the orbital component of the magnetic moment is much more important for the lanthanide ions than for the transition-metal ions.[4] However, less attention has been paid to the magnetic properties of di- or polynuclear lanthanide complexes than to heteronuclear complexes containing 3d−4f metal ions, which results from the difficulties in obtaining pure and well-characterized (f, f′) complexes (f′ being identical or different from f) and in analyzing magnetic behaviors of these complexes, because both orbital contributions of most of the f ions and crystal-field effects have to be considered.[5] In the past years, few homodinuclear lanthanide complexes have been reported and their magnetic behaviors were found to be ferromagnetic or antiferromagnetic interactions between the Ln···Ln ions because of the different bridging ligands or atoms.[6−9]

As a contribution to the understanding of the lanthanide complexes with flexible tripodal ligands, we present herein the synthesis, structural, near-infrared and visible luminescence, and magnetic properties of a series of dinuclear complexes based on the ligand 1,3,5-tris(imidazole-1-ylmethyl)-2,4,6-trimethylbenzene (L), generally formulated as $[Ln_2(L)(HL)(NO_3)_6(HCOO)]\cdot 3CH_3OH$ (Ln = Gd **1**, Tb **2**, Dy **3**, Er **4**, Yb **5**, and Eu 6).

Experimental Section

General Information and Materials. Ligand 1,3,5-tris(imidazole-1-ylmethyl)-2,4,6- trimethylbenzene (L) was synthesized by the method described in the literature.[10] Hydrated lanthanide nitrates were prepared from the corresponding oxides according to literature methods.[11] All chemicals were of reagent-grade quality, obtained from commercial sources, and used as received without further purification. Solvents were purified by standard methods prior to use. Elemental analyses were taken on a Perkin-Elmer 240C elemental analyzer, at the Analysis Center of Nanjing University.

Synthesis of the Complexes. All six complexes were prepared by the same method, as follows: A mixture of $Ln(NO_3)_3\cdot 6H_2O$ (Ln = Gd, Tb, Dy, Er, Yb, and Eu, 0.050 mmol), ligand L (18.0 mg, 0.050 mmol), dried methanol (6.0 mL), and triethyl orthoformate (1.0 mL) was stirred and refluxed for about 2 h. The resulting solution was filtered, and the filtrate was allowed to stand in a desiccator at room temperature for several days. Colorless (pink for complex **4**) block crystals were obtained in ca. 80% yield. Anal. Calcd for $C_{46}H_{62}N_{18}O_{23}Gd_2$, **1**: C, 35.65; H, 4.03; N, 16.27. Found: C, 35.45; H, 3.76; N, 16.52. Anal. Calcd for $C_{46}H_{62}N_{18}O_{23}Tb_2$, **2**: C, 35.58; H, 4.02; N, 16.24. Found: C, 35.34; H, 3.69; N, 16.48. Anal. Calcd for $C_{46}H_{62}N_{18}O_{23}Dy_2$, **3**: C, 35.41; H, 4.01; N, 16.16. Found: C, 34.87; H, 3.88; N, 16.41. Anal. Calcd for $C_{46}H_{62}N_{18}O_{23}Er_2$, **4**: C, 35.20; H, 3.98; N, 16.06. Found: C, 35.16; H, 3.97; N, 16.10. Anal. Calcd for $C_{46}H_{62}N_{18}O_{23}Yb_2$, **5**: C, 34.94; H, 3.95; N, 15.94. Found: C, 34.77; H, 3.49; N, 16.40. Anal. Calcd for $C_{46}H_{62}N_{18}O_{23}Eu_2$, **6**: C, 35.90; H, 4.06; N, 16.38. Found: C, 35.84; H, 3.87; N, 16.28.

X-ray Crystallography. The data collections for complexes **1**−**6** were carried out on a Rigaku RAXIS-RAPID Imaging Plate diffractometer using graphite-monochromated Mo Kα radiation (λ = 0.71075 Å) at 200 K. The structures were solved by the direct method with SIR92[12] and expanded using Fourier techniques.[13] All data were refined anisotropically by the full-matrix least-squares method for non-hydrogen atoms. The hydrogen atom (H1) of the protonated imidazole group was located in a difference Fourier map directly, and the other hydrogen atoms were generated geometrically. All calculations were carried out on an SGI workstation using the teXsan crystallographic software package by the Molecular Structure corporation.[14] Details of the crystal parameters, data collection, and refinements for complexes **1**−**6** are summarized in Table 1. Selected bond lengths and angles with their estimated

(3) Representative recent papers describing NIR luminescence from lanthanide complexes: (a) Voloshin, A. I.; Shavaleev, N. M.; Kazakov, V. P. *J. Lumin.* **2001**, *93*, 199. (b) Faulkner, S.; Beeby, A.; Carrie, M. C.; Dadabhoy, A.; Kenwright, A. M.; Sammes, P. G. *Inorg. Chem. Commun.* **2001**, *4*, 187. (c) Silva, F. R. G. E.; Malta, O. L.; Reinhard, C.; Güdel, H. U.; Piguet, C.; Moser, J. E.; Bünzli, J.-C. G.; *J. Phys. Chem.* A **2002**, *106*, 1670. (d) Dickins, R. S.; Aime, S.; Batsanov, A. S.; Beeby, A.; Botta, M.; Bruce, J.; Howard, J. A. K.; Love, C. S.; Parker, D.; Peacock, R. D.; Buschmann, H. *J. Am. Chem. Soc.* **2002**, *124*, 12697. (e) Hebbink, G. A.; Klink, S. I.; Grave, L.; Oude Alink, P. G. B.; van Veggel, F. C. J. M. *ChemPhysChem* **2002**, *3*, 1014. (f) Faulkner, S.; Pope, S. J. A. *J. Am. Chem. Soc.* **2003**, *125*, 10526. (g) Hasegawa, Y.; Sogabe, K.; Wada, Y.; Yanagida, S. *J. Lumin.* **2003**, *101*, 235. (h) Shavaleev, N. M.; Accorsi, G.; Virgili, D.; Bell, Z. R.; Lazarides, T.; Calogero, G.; Armaroli, N.; Ward, M. D. *Inorg. Chem.* **2005**, *44*, 61.

(4) Benelli, C.; Gatteschi, D. *Chem. Rev.* **2002**, *102*, 2369.

(5) (a) Kahn, M. L.; Ballou, R.; Porcher, P.; Kahn, O.; Sutter, J.-P. *Chem.—Eur. J.* **2002**, *8*, 525. (b) Costes, J.-P.; Juan, J.-M. C.; Dahan, F.; Nicodème, F. *J. Chem. Soc., Dalton Trans.* **2003**, 1272. (c) Zhao, B.; Cheng, P.; Dai, Y.; Liao, D.-Z.; Yan, S.-P.; Jiang, Z.-H.; Wang, G.-L. *Angew. Chem., Int. Ed.* **2003**, *42*, 934.

(6) (a) Kahwa, I. A.; Folkes, S.; Williams, D. J.; Ley, S. V.; O'Mahoney, C. A.; McPherson, C. L. *J. Chem. Soc., Chem. Commun.* **1989**, 1531. (b) Liu, S.; Gelmini, L.; Rettig, S. J.; Thompson, R. C.; Orvig, C. *J. Am. Chem. Soc.* **1992**, *114*, 6081. (c) Panagiotopoulos, A.; Zafiropoulos, T. F.; Perlepes, S. P.; Bakalbassis, E.; Masson-Ramade, I.; Kahn, O.; Terzis, A.; Raptopoulou, C. P. *Inorg. Chem.* **1995**, *34*, 4918.

(7) (a) Costes, J.-P.; Clemente-Juan, J. M.; Dahan, F.; Nicodème, F.; Verelst, M. *Angew. Chem., Int. Ed.* **2002**, *41*, 323. (b) Hernández-Molina, M.; Lorenzo-Luis, P. A.; López, T.; Ruiz-Pérez, C.; Lloret, F.; Julve, M. *CrystEngComm* **2000**, *31*, 1. (c) Costes, J.-P.; Dahan, F.; Dupuis, A.; Lagrave, S.; Laurent, J.-P. *Inorg. Chem.* **1998**, *37*, 153. (d) Costes, J.-P.; Dupuis, A.; Lauurent, J.-P. *Inorg. Chim. Acta* **1998**, *268*, 125.

(8) (a) Niu, S. Y.; Jin, J.; Jin, X. L.; Yang, Z. Z. *Solid State Sci.* **2002**, *4*, 1103. (b) Hou, H.; Li, G.; Li, L.; Zhu, Y.; Meng, X.; Fan, Y. *Inorg. Chem.* **2003**, *42*, 428.

(9) (a) Gheorghe, R.; Kravtsov, V.; Simonov, Y. A.; Costes, J.-P.; Journaux, Y.; Andruh, M. *Inorg. Chim. Acta* **2004**, *357*, 1613. (b) Ishikawa, N.; Otsuka, S.; Kaizu Y. *Angew. Chem., Int. Ed.* **2005**, *44*, 731.

(10) Liu, H.-K.; Sun, W.-Y.; Zhu, H.-L.; Yu, K.-B.; Tang, W. X. *Inorg. Chim. Acta* **1999**, *295*, 129.

(11) Bünzli, J.-C. G.; Chopin, G. R. *Lanthanide Probes in Life, Chemical and Earth Sciences: Theory and Practice*; Elsevier: Amsterdam, 1989.

(12) Altomare, A.; Cascarano, G.; Giacovazzo, C.; Guagliardi, A. *SIR92*; *J. Appl. Crystallogr.* **1993**, *26*, 343.

(13) Beurskens, P. T.; Admiraal, G.; Beurskens, G.; Bosman, W. P.; de Gelder, R.; Israel, R.; Smits, J. M. M. *The DIRDIF-94 Program System*; Technical Report of the Crystallography Laboratory, University of Nijmegen: Nijmegen, The Netherlands, 1994.

(14) *teXsan: Crystal Structure Analysis Package*; Molecular Structure Corporation: The Woodlands, TX, 1999.

Table 1. Crystal Data and the Structure Refinement for Complexes **1**−**6**

	1	**2**	**3**
formula	$C_{46}H_{62}N_{18}O_{23}Gd_2$	$C_{46}H_{62}N_{18}O_{23}Tb_2$	$C_{46}H_{62}N_{18}O_{23}Dy_2$
formula wt	1549.64	1552.98	1560.14
cryst syst	orthorhombic	orthorhombic	orthorhombic
space group	*Pnnm*	*Pnnm*	*Pnnm*
a (Å)	19.551(10)	19.545(17)	19.492(10)
b (Å)	18.916(9)	18.877(14)	18.875(10)
c (Å)	16.924(8)	16.840(14)	16.854(7)
V (Å^3)	6259(5)	6213(9)	6201(5)
Z	4	4	4
T (K)	200	200	200
λ (Å)	0.71075	0.71075	0.71075
ρ_{calcd} (g cm^{-3})	1.645	1.660	1.671
μ (mm^{-1})	2.190	2.348	2.481
F(000)	3104	3112	3120
θ range/deg	3.00/27.48	3.00/27.49	3.20/27.48
no. of reflns collected	59136	61025	59991
no. of independent reflns	7413	7369	7348
no. of restraints/params	24/443	1/443	12/443
GOF on F^2	0.995	0.858	0.951
R_{int}	0.0362	0.0588	0.0458
R1 [$I > 2\sigma(I)$]	0.0263	0.0291	0.0250
wR2 (all data)	0.0613	0.0565	0.0526
	4	**5**	**6**
formula	$C_{46}H_{62}N_{18}O_{23}Er_2$	$C_{46}H_{62}N_{18}O_{23}Yb_2$	$C_{46}H_{62}N_{18}O_{23}Eu_2$
formula wt	1569.66	1581.22	1539.06
cryst syst	orthorhombic	orthorhombic	orthorhombic
space group	*Pnnm*	*Pnnm*	*Pnnm*
a (Å)	19.504(15)	19.453(11)	19.543(18)
b (Å)	18.595(12)	18.557(10)	18.936(14)
c (Å)	16.761(14)	16.768(8)	16.897(13)
V (Å^3)	6079(8)	6053(6)	6253(9)
Z	4	4	4
T (K)	200	200	200
λ (Å)	0.71075	0.71075	0.71075
ρ_{calcd} (g cm^{-3})	1.715	1.735	1.635
μ (mm^{-1})	2.834	3.163	2.077
F(000)	3136	3152	3096
θ range/deg	3.03/27.48	3.03/27.48	3.00/27.48
no. of reflns collected	54093	57822	60646
no. of independent reflns	7175	7168	7413
no. of restraints/params	6/454	24/444	24/444
GOF on F^2	0.906	0.802	1.001
R_{int}	0.0928	0.1201	0.0639
R1 [$I > 2\sigma(I)$]	0.0351	0.0357	0.0297
wR2 (all data)	0.0437	0.0346	0.0499

[a] $R = \sum||F_o| - |F_c||/\sum|F_o|$. [b] $wR = |\sum w(|F_o|^2 - |F_c|^2)|/\sum|w(F_o)^2|^{1/2}$, where $w = 1/[\sigma^2(F_o^2) + (aP)^2 + bP]$. $P = (F_o^2 + 2F_c^2)/3$.

Table 2. Selected Bond Distances (Å) and Angles (deg) for Complex **1**

Gd−O1	2.340(2)	Gd−O11	2.473(3)	Gd−O12	2.470(2)
Gd−O21	2.516(2)	Gd−O22	2.459(2)	Gd−O31	2.453(2)
Gd−O32	2.492(2)	Gd−N32	2.484(3)	Gd−N132	2.490(3)
O1−Gd−O11	147.66(9)	O1−Gd−O12	150.82(8)	O1−Gd−O21	72.79(7)
O1−Gd−O22	124.14(7)	O1−Gd−O31	85.25(8)	O1−Gd−O32	78.74(8)
O1−Gd−N32	84.48(8)	O1−Gd−N132	77.96(8)	O11−Gd−O12	51.78(9)
O11−Gd−O21	123.20(8)	O11−Gd−O22	76.16(9)	O11−Gd−O31	125.21(9)
O11−Gd−O32	110.05(8)	O11−Gd−N32	73.96(8)	O11−Gd−N132	75.38(9)
O12−Gd−O21	118.12(9)	O12−Gd−O22	73.53(9)	O12−Gd−O31	74.16(9)
O12−Gd−O32	72.32(9)	O12−Gd−N32	123.55(9)	O12−Gd−N132	96.73(9)
O21−Gd−O22	51.46(8)	O21−Gd−O31	71.89(8)	O21−Gd−O32	118.27(8)
O21−Gd−N32	76.77(8)	O21−Gd−N132	145.03(8)	O22−Gd−O31	81.23(9)
O22−Gd−O32	127.64(8)	O22−Gd−N32	80.25(8)	O22−Gd−N132	149.58(8)
O31−Gd−O32	51.91(8)	O31−Gd−N32	148.64(8)	O31−Gd−N132	124.62(9)
O32−Gd−N32	152.10(8)	O32−Gd−N132	73.05(8)	N32−Gd−N132	81.79(9)

standard deviations for complex **1** are listed in Table 2; those of other complexes are listed in Table S1 in the Supporting Information.

Luminescence and Magnetic Measurements. Samples for luminescence measurements of the lanthanide(III) complexes in organic media were prepared under deoxygenated conditions. Solutions (1 mM) of the complexes were prepared in 5 mL of DMSO-d_6 and then transferred to a quartz cell for optical measurements (optical path length 10 mm). Solid-state luminescences of the complexes were measured using a cylindrical quartz cell (diameter: 1 mm). Emission and excitation spectra were measured at room temperature using a JOBIN YVON/HORIBA SPEX

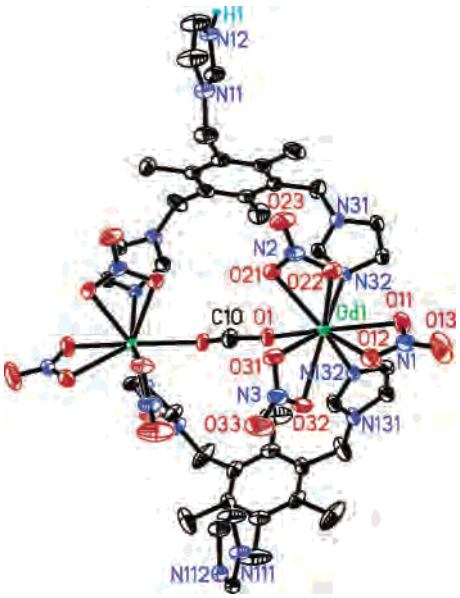

Figure 1. ORTEP plots of **1** showing the local coordination environment of Gd(III) with thermal ellipsoids at the 30% level of probability.

Fluorolog t3 system (slit: 0.1 nm). The spectra were corrected for detector sensitivity and lamp intensity variations. Emission lifetimes were measured using the SPEX Fluorolog t3 system (slit: 0.5 nm) with a SPEX Phosphorimeter 1934D (flush lamp pulse: 0.04 ms). Variable-temperature magnetic susceptibility measurements were performed on a SQUID MPMS-XL7 in an applied field of 2000 G using crystalline samples of **1**−**6** in the range 300−1.8 K. The magnetic susceptibilities of all complexes are corrected by Pascal's constant and the diamagnetism of holder.

Results and Discussion

Description of Crystal Structures. Previous studies showed that flexible tripodal ligands with aromatic core are versatile and can form various MOFs with novel structures and interesting properties by reactions with varied transition-metal salts.[15] When the construction of MOFs was carried out by using lanthanide nitrate salts [$Ln(NO_3)_3 \cdot 6H_2O$, Ln = Gd, Tb, Dy, Er, Yb, and Eu] and 1,3,5-tris(imidazole-1-ylmethyl)- 2,4,6-trimethylbenzene (L) in the presence of triethyl orthoformate, which was used as a dehydrating reagent considering the lanthanide ions have a higher affinity for oxygen atoms than nitrogen atoms, complexes **1**−**6** were successfully isolated and characterized. As evidenced by the X-ray crystallographic analyses, the space group and cell parameters similar to those listed in Table 1 indicate that these six complexes are isomorphous and isostructural, and thus only the structure of complex **1** is described here in detail. The complex consists of two Gd(III) atoms, two L ligands, six nitrate anions, and one formate group, as illustrated in Figure 1. The formate group comes from the hydrolysis of the triethyl orthoformate. Each Gd(III) atom is nine-coordinated, in which two nitrogen atoms are from two imidazolyl groups of two different L ligands with a N32−Gd−N132 angle of 81.79(9)° and Gd−N bond lengths in the range 2.484(3)−2.490(3) Å. Six oxygen atoms come from three bidentate-chelating nitrate anions and one oxygen atom comes from the formate group, with O−Gd−O bond angles varying from 51.46(8) to 149.58(8)° and Gd−O bond distances in the range of 2.340(2) to 2.516(2) Å, as listed in Table 2.

It is noteworthy that in this complex, each L acts as a bidentate-bridging ligand to connect two metal atoms using two of its three imidazole groups, whereas the third imidazole group is free of coordination. Furthermore, one L ligand adopts a cis, cis, cis conformation and the other adopts a cis, trans, trans conformation in which the uncoordinated imidazole group is protonated. Two metal atoms are further linked by the formate group to form a bowl-like architecture in which the dihedral angle between the benzene rings of the two ligands is 70.3°. The vacancy of the bowl is occupied by three methanol molecules, as shown in Figure S1 of the Supporting Information. Such bowl-like dinuclear molecules are connected together by hydrogen bonds (listed in Table S2 of the Supporting Information), giving a 2D network (Figure S2 of the Supporting Information) and further resulting in a 3D structure via $\pi-\pi$ interactions (Figure S3 of the Supporting Information; the distance of centriod−centriod separations of benzene rings from two adjacent layers are also listed in Table S2 of the Supporting Information).

Photoluminescence Properties. Studies on luminescence lanthanides have concentrated on europium, terbium, samarium, and dysprosium ions in the visible region; the main work has dealt with europium and terbium complexes, which have long (millisecond order) luminescence lifetimes that are easy to detect and measure. More recently, a number of groups have begun to exploit the developments in detection of near-infrared luminescence to study the luminescence from neodymium, erbium, and ytterbium complexes, which may be applied in assays. Therefore, the luminescence properties of complexes **2**−**6** were studied in the powder solid state and/or in DMSO-d_6 solutions at room temperature.

When europium complex **6** was measured in the solid state and in DMSO-d_6 solution under excitation with 394 nm, a very intense band at 616 nm arising from the $^5D_0 \rightarrow {}^7F_2$ transition was recorded, and its luminescence spectra are depicted in Figure 2a. Another three bands at 590, 651, and 698 nm correspond to transitions from the $^5D_0$ state to the $^7F_1$, $^7F_3$, and $^7F_4$ levels, respectively. It is known that the $^5D_0 \rightarrow {}^7F_2$ transition induced by the electric dipole moment is hypersensitive to the coordination environment of the Eu(III) ion, whereas the $^5D_0 \rightarrow {}^7F_1$ transition is a magnetic dipole in origin and less sensitive to its environment.[16] Thus, the spectra were normalized with respect to the $^5D_0 \rightarrow {}^7F_1$

(15) For examples: (a) Fan, J.; Sui, B.; Okamura, T.-a.; Sun, W.-Y.; Tang, W.-X.; Ueyama, N. *J. Chem. Soc., Dalton Trans.* **2002**, 3868. (b) Fan, J.; Sun, W.-Y.; Okamura, T.-a.; Xie, J.; Tang, W.-X.; Ueyama, N. *New J. Chem.* **2002**, *26*, 199. (c) Fan, J.; Zhu, H.-F.; Okamura, T.-a.; Sun, W.-Y.; Tang, W.-X.; Ueyama, N. *Chem.—Eur. J.* **2003**, *9*, 4724. (d) Fan, J.; Zhu, H.-F.; Okamura, T.-a.; Sun, W.-Y.; Tang, W.-X.; Ueyama, N. *Inorg. Chem.* **2003**, *42*, 158.

(16) (a) Hasegawa, Y.; Yamamuro, M.; Wada, Y.; Kanehisa, N.; Kai, Y.; Yanagida, S. *J. Phys. Chem. A* **2003**, *107*, 1697. (b) Hasegawa, Y.; Iwamuro, M.; Murakoshi, K.; Wada, Y.; Arakawa, R.; Yamanaka, T.; Nakashima, N.; Yanagida, S. *Bull. Chem. Soc. Jpn.* **1998**, *71*, 2573. (c) Hasegawa, Y.; Wada, Y.; Yanagida, S. *J. Photochem. Photobiol., C: Photochem. Rev.* **2004**, *5*, 183.

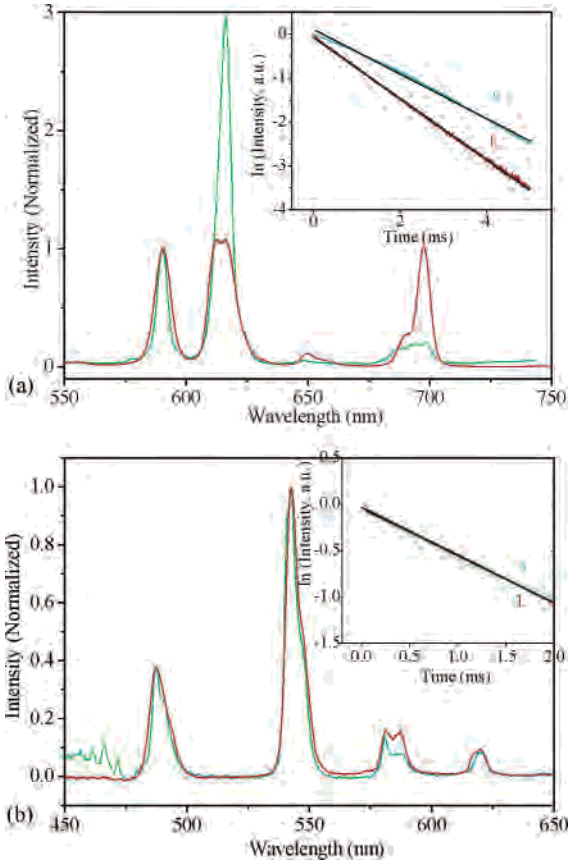

Figure 2. Emission spectra in the solid state (green line) and in DMSO-d_6 solution (red line) for (a) Eu(III) complex and (b) Tb(III) complex. The spectra were normalized at the $^5D_0 \rightarrow {}^7F_1$ magnetic dipole transition for the Eu(III) complex and at the $^5D_4 \rightarrow {}^7F_5$ for the Tb(III) complex. Inset: luminescence decay curves for the complex in the solid state (S) and in DMSO-d_6 solution (L). The black solid lines are the best fits of experimental data.

transition. For complex **6**, the ratio I ($^5D_0 \rightarrow {}^7F_2/{}^5D_0 \rightarrow {}^7F_1$) is equal to 2.96 in the solid state, which indicates that the Eu(III) ion has a lower symmetric coordination environment close to a $D2$ symmetry.[17] This is in agreement with the result of the structural analysis of the complex. However, the $^5D_0 \rightarrow {}^7F_2$ transition intensity decreases, and the ratio I of complex **6** in DMSO-d_6 solution is smaller than that of the complex in the solid state, which was probably caused by the DMSO solvent, and the results indicate that the photoluminescence property of the Eu(III) complex is sensitive to its environment.[18]

The emission decay profiles of Eu(III) complex **6** in powder and in DMSO-d_6 were also measured (Figure 2a, inset). The single-exponential decay profile of the Eu(III) complex indicates the presence of a single-luminescence species and homogeneity of the sample.[19] The emission lifetime for the Eu(III) complex in DMSO-d_6 (1.45 ms) is shorter than that in the solid state (1.9 ms), which also shows

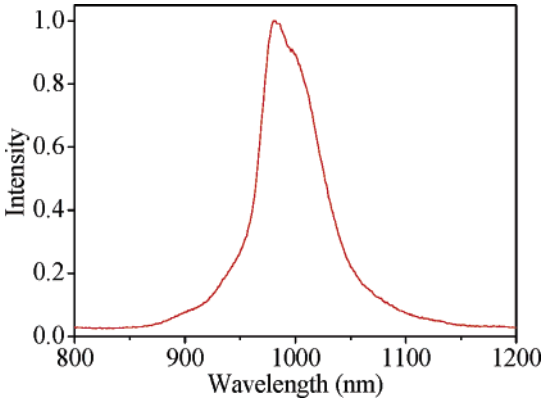

Figure 3. Near-infrared emission spectrum of the Yb(III) complex in DMSO-d_6 (1 mM) upon excitation at 290 nm.

that the Eu(III) ion is a sensitive luminescence probe for the Eu^{3+} site in europium complexes.[20]

As exhibited in Figure 2b, complex **2** gave typical Tb(III) emission spectra containing the expected sequence of $^5D_4 \rightarrow {}^7F_J$ ($J = 3-6$) transitions both in the powder sample and in DMSO-d_6 solution upon excitation at 370 nm. The spectra are dominated by the $^5D_4 \rightarrow {}^7F_5$ transition, peaking at 542 nm, which gave an intense green luminescence output for the sample. The lifetimes of complex **2** are 2.0 and 1.94 ms for the powder and solution samples, respectively, and their experimental curves also fit well with single-exponential decays (Figure 2b, inset) at ambient temperature. The very similar emission spectra and decay profiles for **2** in the solid state and in solution indicate that Tb(III) is less sensitive to its environment.

The luminescence properties of complexes **3** and **4** were also measured, but no emissions were observed.

When complex **5** was excited at 290 nm in DMSO-d_6 solution, it led to a typical metal-centered near-infrared luminescence at 980 nm (Figure 3). Ytterbium(III) is a special case among the near-infrared-emitting lanthanide ions, because the Yb(III) ion has only one excited 4f level, namely, the $^2F_{5/2}$ level, so its luminescence observed at 980 nm is assigned to the $^2F_{5/2} \rightarrow {}^2F_{7/2}$ transition.

The mechanism of energy transfer from the ligand to the metal has been widely discussed to interpret the luminescence of lanthanide complexes.[21] When the triplet-state energy of the ligand is greater than or equal to the energy gap (ΔE) between the excited state and ground state of the metal ion, efficient luminescence could be obtained.[21] From the results discussed above, we could presume that the energy gap (ΔE) of Dy(III) and Er(III) ions may be smaller than that of Eu(III), Tb(III), and Yb(III), which is also consistent with the reported complexes.[21a]

Magnetic Properties. As the smallest carboxylate, the formate ion has been observed to adopt different bridging

(17) (a) Horrocks, W. d. W., Jr.; Sudnick, D. R. *Acc. Chem. Res.* **1981**, *14*, 384. (b) Choppin, G. R.; Peterman, D. R. *Coord. Chem. Rev.* **1998**, *174*, 283.
(18) Nakamura, K.; Hasegawa, Y.; Wada, Y.; Yanagida, S. *Chem. Phys. Lett.* **2004**, *398*, 500.
(19) Liu, C.-B.; Sun, C.-Y.; Jin, L.-P.; Lu, S.-Z. *New J. Chem.* **2004**, *28*, 1019.
(20) (a) Horrocks, W. H., Jr.; Bolender, J. P.; Smith, W. D.; Supkowsky, R. M. *J. Am. Chem. Soc.* **1997**, *119*, 5972. (b) Driesen, K.; Deun, R. V.; Görller-Walrand, C.; Binnemans, K. *Chem. Mater.* **2004**, *16*, 1531.
(21) (a) Stein, G.; Würzberg, E. *J. Chem. Phys.* **1975**, *62*, 208. (b) Supkowski, R. M.; Bolender, J. P.; Smith, W. D.; Reynolds, L. E. L.; Horrocks, W. Dew. *Coord. Chem. Rev.* **1999**, *185−186*, 307. (c) Beeby, A.; Faulkner, S.; Parker, D.; Williams, J. A. G. *J. Chem. Soc., Perkin Trans.* **2001**, *2*, 1268.

Scheme 1

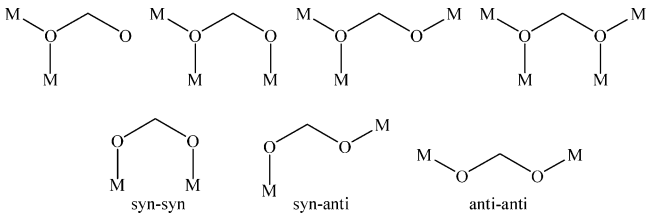

modes (see Scheme 1), such as syn−syn, anti−anti, syn−anti, and monatomic, to link two or more metal ions and to form a variety of zero-, one-, two-, and three-dimensional complexes,[22] and they mediate ferro- or antiferromagnetic coupling between the metal ions in different situations.[23] According to the structural data described above, each formate group in **1**−**6** connects two metal atoms with the anti−anti mode, similar to many reported compounds with formate as the bridging ligand (Figure 1), thus it is interesting to perform magnetic studies that evaluate the eventual exchange interactions between the metal centers. Generally speaking, the carboxylate group in the anti−anti mode favors the antiferromagnetic coupling between the spin carriers. However, when variable-temperature magnetic susceptibility measurements of **1**−**6** were performed in the range 300−1.8 K, the results showed that their magnetic properties are very different, although they have the same structure. Figures 4−6 show the temperature dependence of the magnetic susceptibility in the form of $\chi_M T$ vs T for complexes **1** (Gd) (Figure 4); **2** (Tb), **3** (Dy), and **4** (Er) (Figure 5); and **5** (Yb) and **6** (Eu) (Figure 6), respectively. The field dependence of magnetization at 1.8 K for complexes **1**−**6** is provided in the Supporting Information (Figures S4,−S6).

For complex **1**, in the whole temperature range, the $\chi_M T$ value is almost constant from 15.50 emu K mol^{-1} at room temperature to 15.64 emu K mol^{-1} at 9 K, and then to 14.7 emu K mol^{-1} at 2 K (Figure 4). Above 9 K, $\chi_M T$ slightly increases as the temperature decreases, suggesting very weak ferromagnetic coupling mediated by the formate group between the Gd(III) ions. Below 9 K, $\chi_M T$ decreases with cooling, indicating the presence of possible antiferromagnetic interactions between the dinuclear molecules. For estimating these magnetic interactions, the simple dimer model with

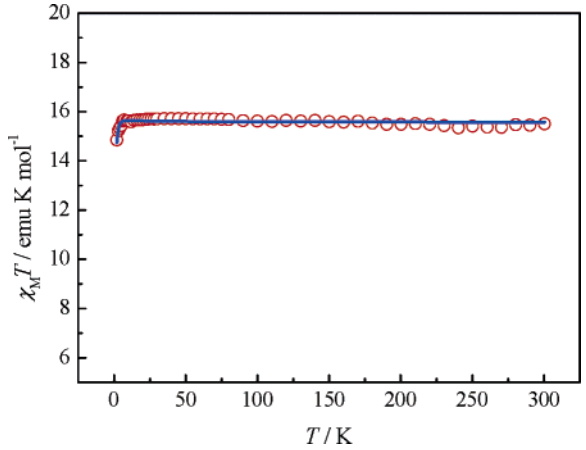

Figure 4. Temperature dependence of magnetic susceptibilities in the form of $\chi_M T$ at an applied field of 2 kOe from 2 to 300 K for complex **1** (○). The solid line is the fitting results.

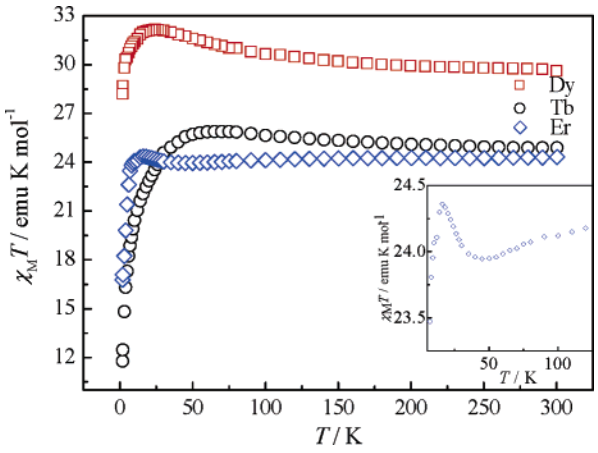

Figure 5. Temperature dependence of magnetic susceptibilities in the form of $\chi_M T$ at an applied field of 2 kOe from 1.8 to 300 K for complexes **2** (○), **3** (□), and **4** (◇). Inset: a zoom of $\chi_M T$ vs T plot in the range 5−125 K for **4**.

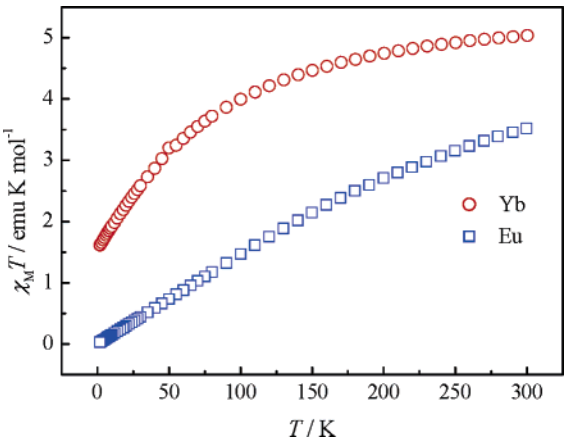

Figure 6. Temperature dependence of magnetic susceptibilities in the form of $\chi_M T$ at an applied field of 2 kOe from 1.8 to 300 K for complexes **5** (○) and **6** (□).

Hamiltonian $\mathbf{H} = -2JS_AS_B$ and $S_A = S_B = 7/2$, as reported previously, [6c,7a] can be used here. The expression of the magnetic susceptibility of complex **1** is

$$\chi_M = \frac{2Ng^2\beta^2}{kT}\frac{A}{B} \qquad (1)$$

(22) For examples: (a) Martin, R. L.; Waterman, H. *J. Chem. Soc.* **1959**, 1359. (b) Okada, K.; Kay, M. I.; Cromer, D. T.; Almodovar, I. *J. Chem. Phys.* **1966**, *44*, 1648. (c) Cotton, F. A.; Rice, G. W. *Inorg. Chem.* **1978**, *17*, 688. (d) Armstrong, W. H.; Spool, A.; Papaefthymiou, G. C.; Frankel, R. B.; Lippard, S. J. *J. Am. Chem. Soc.* **1984**, *106*, 3653. (e) Sessler, J. L.; Hugdahl, J. D.; Lynch, V.; Davis, B. *Inorg. Chem.* **1991**, *30*, 334. (f) Fujino, M.; Achiwa, N.; Koyano, N.; Shibuya, I.; Ridwan; Yamagata, K. *J. Magn. Magn. Mater.* **1992**, *104*−*107*, 851. (g) Escrivà, E.; Carrió, J. S.; Lezama, L.; Folgado, J. V.; Pezarro, J. L.; Ballesteros, R.; Abarca, B. *J. Chem. Soc., Dalton Trans.* **1997**, 2033. (h) Cornia, A.; Caneschi, A.; Dapporto, P.; Faberetti, A. C.; Gatteschi, D.; Malevasi, W.; Sangregorio, C.; Sessoli, R. *Angew. Chem., Int. Ed.* **1999**, *38*, 1780. (i) Cadiou, C.; Coxall, R. A.; Graham, A.; Harrison, A.; Helliwell, M.; Parsons, S.; Winpenny, R. E. P. *Chem. Commun.* **2002**, 1106. (j) Wang, Z.-M.; Zhang, B.; Fujiwara, H.; Kobayashi, H.; Kurmoo, M. *Chem. Commun.* **2004**, 416.

(23) (a) Pérez, C. R.; Sanchiz, J.; Molina, M. H.; Lloret, F.; Julve, M. *Inorg. Chem.* **2000**, *39*, 1363. (b) Colacio, E.; Ghaze, M.; Kivekäs, R.; Moreno, J. M. *Inorg. Chem.* **2000**, *39*, 2882. (c) Yolanda, R. M.; Catalina, R. P.; Joaquin, S.; Francesc, L.; Miguel, J. *Inorg. Chim. Acta* **2001**, *318*, 159. (d) Wang, X.-Y.; Gan, L.; Zhang, S.-W.; Gao, S. *Inorg. Chem.* **2004**, *43*, 4615.

where

$$A = 140e^{56J/kT} + 91e^{42J/kT} + 55e^{30J/kT} + 30e^{20J/kT} + 14e^{12J/kT} + 5e^{6J/kT} + e^{2J/kT}$$

$$B = 15e^{56J/kT} + 13e^{42J/kT} + 11e^{30J/kT} + 9e^{20J/kT} + 7e^{12J/kT} + 5e^{6J/kT} + 3e^{2J/kT} + 1$$

and N, g, and β have their usual meanings. J is the coupling constant between the Gd(III) ions. When zj' is regarded as the interdimer interaction, eq 1 can be rewritten as the following

$$\chi = \frac{\chi_M}{1 - (2zj'/Ng^2\beta^2)\chi_M} \quad (2)$$

The best fit by a standard squares-fitting program gives $g = 1.989(1)$, $J = 0.045(4)$ cm^{-1}, $zj' = -0.019(1)$ cm^{-1}, and $R = 5.7 \times 10^{-4}$.

For complexes **2**−**6**, compared with **1**, it is very difficult to analyze their magnetic properties because of the orbital contribution. Usually, the spin−orbital coupling leads the $4f^n$ configuration of Ln(III) ions, except for Gd(III), to split into $^{2S+1}L_J$ states, and the latter further splits into Stark components under the crystal-field perturbation.[11,24] Thus, the variable-temperature magnetic properties of a free ion of a rare earth metal generally shows strong deviations from the Curie law, and $\chi_M T$ decreases with the cooling temperature because of the depopulation of Stark levels. However, as illustrated in Figure 5, complexes **2**−**4** obviously show ferromagnetic coupling between lanthanide ions. Complexes **2** and **3** exhibit similar magnetic properties. As an example, for complex **2**, the $\chi_M T$ value is 24.90 emu K mol^{-1} at room temperature, which is slightly higher than the value of 23.625 emu K mol^{-1} expected for two independent Tb(III) ions, including the significant contribution of the 4f orbital ($4f^8$, $J = 6$, $S = 3$, $L = 3$, $g = 1.5$, $^7F_6$). As the temperature decreases, $\chi_M T$ gradually increases, reaching 25.88 emu K mol^{-1} at 65 K, and then abruptly decreases to 11.78 emu K mol^{-1} at 1.8 K. This magnetic behavior indicates ferromagnetic coupling mediated by the formate group between the Tb(III) ions in complex **2**, and the coupling interaction is high enough to compensate for the depopulation of the Stark levels, but that the maximum of $\chi_M T$ is only slightly higher than the value at room-temperature implies that the ferromagnetic coupling is very weak.

For complex **4**, the magnetic property from the $\chi_M T$ vs T curve seems more complicated than those of **2** and **3**. As shown in Figure 5, the $\chi_M T$ curve of complex **4** slowly decreases from 24.31 emu K mol^{-1} at 300 K to a minimum of 23.94 emu K mol^{-1} at 45 K with cooling (Figure 5, inset) and then gradually increases, reaching a maximum of 24.36 emu K mol^{-1} at 16 K, and subsequently goes down sharply to 16.77 emu K mol^{-1} at 1.8 K. Such magnetic behavior of a dinuclear Er(III) complex has been recently reported for $[ErL_3(H_2O)_2]_2 \cdot 4H_2O$ (HL = salicylic acid) by Costes et al.[7a] The temperature dependence of magnetic behavior also indicates ferromagnetic coupling between the Er(III) ions in complex **4**, but the coupling interaction cannot completely compensate for the depopulation of the Stark levels such as can be done in complexes **2** and **3**;[25] $\chi_M T$ decreases with the cooling system, and a minimum was observed.

Complexes **5** and **6** display magnetic behavior that is very different from that of complexes **1**−**4**, as shown in Figure 6. For complex **5**, $\chi_M T$ is 5.02 emu K mol^{-1} at 300 K, which is slightly less than the theoretical value of 5.14 emu K mol^{-1} on the basis of two independent Yb(III) ions with a $^2F_{7/2}$ ground multiplet, and it monotonically decreases with cooling temperature, indicating that the depopulation of the Stark levels possibly dominates the magnetic properties in complex **5**. For complex **6**, at 300 K, the $\chi_M T$ value is equal to 3.52 emu K mol^{-1}, which corresponds to the population of an excited state (the theoretical value is 3 emu K mol^{-1}) on the basis of two Eu(III) ions. As the temperature cools, $\chi_M T$ decreases and is close to zero at 1.8 K, indicating a ground state of $^7F_0$ for Eu(III) ions.

Conclusion

A series of dinuclear complexes with the general formula $[Ln_2(L)(HL)(NO_3)_6(HCOO)] \cdot 3CH_3OH$ (Ln = Gd, Tb, Dy, Er, Yb, and Eu) was synthesized, and single-crystal X-ray diffraction analysis revealed that six complexes are isomorphous and isostructural. The studies of luminescence properties showed that Eu(III) and Tb(III) complexes exhibited typical luminescence in the visible region, respectively; the Yb(III) compound emitted typical near-infrared luminescence in DMSO-d_6 solution, whereas no emissions were observed for the Dy(III) and Er(III) complexes. Magnetic studies revealed that the Gd(III) complex is nearly a paramagnet, and the ferromagnetic interactions appear in the Tb(III), Dy(III), and Er(III) complexes; however, the depopulation of Stark levels in Yb(III) and Eu(III) complexes dominates the magnetic properties in the whole temperature range.

Acknowledgment. This work was supported by the National Natural Science Foundation of China (Grant 20231020) and the National Science Fund for Distinguished Young Scholars (Grant 20425101).

Supporting Information Available: X-ray crystallographic file in CIF format; selected bond lengths and angles for **2**−**6** (Table S1); hydrogen bonding and $\pi-\pi$ interactions (Table S2); side-view, 2D, and 3D structure of **1** (Figures S1−S3); and field dependence of magnetization (Figures S4−S6). This material is available free of charge via the Internet at http://pubs.acs.org.

IC0518071

(24) Costes, J.-P.; Nicodème, F. *Chem.—Eur. J.* **2002**, *8*, 3442.

(25) (a) Kou, H.-Z.; Zhou, B.-C.; Wang, R.-J. *Inorg. Chem.* **2003**, *42*, 7658. (b) Zheng, X.-J.; Wang, Z.-M.; Gao, S.; Liao, F.-H.; Yan, C.-H.; Jin, L.-P. *Eur. J. Inorg. Chem.* **2004**, 2968. (c) He, Z.; Gao, E.-Q.; Wang, Z.-M.; Yan, C.-H.; Kurmoo, M. *Inorg. Chem.* **2005**, *44*, 862.